A photoprotection strategy for microsecond-resolution single-molecule fluorescence spectroscopy

Luis A Campos[1,2,4], Jianwei Liu[2–4], Xiang Wang[2,3], Ravishankar Ramanathan[1], Douglas S English[2,3] & Victor Muñoz[1,2]

Time resolution of current single-molecule fluorescence techniques is limited to milliseconds because of dye blinking and bleaching. Here we introduce a photoprotection strategy that affords microsecond resolution by combining efficient triplet quenching by oxygen and Trolox with minimized bleaching via the oxygen radical scavenger cysteamine. Using this approach we resolved the single-molecule microsecond conformational fluctuations of two proteins: the two-state folder α-spectrin SH3 domain and the ultrafast downhill folder BBL.

© 2011 Nature America, Inc. All rights reserved.

Single-molecule methods are quickly becoming the gold standard for the study of biological processes controlled by macromolecules[1]. The great advantage of these methods is that they report on the stochastic fluctuations that are key to biological mechanisms and, if sufficiently fast, reveal macromolecule dynamics directly without the need to synchronize large ensembles and interpret relaxation decays in kinetic terms. Single-molecule fluorescence spectroscopy (and particularly single-molecule fluorescence resonance energy transfer (FRET)) is ideally suited for the study of RNA-folding[2] and protein-folding[3] reactions because it can potentially resolve any conformational fluctuation that affects the distance between the donor and acceptor dyes. However, the ultimate temporal and statistical (shot noise) resolution is determined by the photon count rate that can be detected from individual fluorescent dyes. Given current instrument collection efficiencies (~1%)[4] and fluorescence lifetimes of single-molecule FRET dyes (~3 ns), the theoretical maximum photon count rate is ~3 MHz, which amounts to 10-μs resolution because measuring FRET efficiencies precisely requires at least 30 photons. However, current single-molecule FRET dyes saturate near 100 kHz (ref. 5), limiting the practical resolution to milliseconds[2]. This restriction impedes resolving processes that involve sub-millisecond macromolecule conformational dynamics.

Photon emissions saturate early because under high irradiance the dyes undergo transient blinking. The most general of the blinking mechanisms is formation of triplet states, which have microsecond lifetimes and thus deplete the ground state for further excitations. Furthermore, high irradiance bleaches the dye by photo-oxidation, also reducing the total photon output. To reach microsecond resolution in single-molecule FRET, it is thus critical to reduce blinking and bleaching. A common strategy is to eliminate oxygen in solution with enzymatic antioxidants combined with organic triplet quenchers, such as 6-hydroxy-2,5,7,8-tetramethylchroman-2-carboxylic acid (Trolox)[6]. However, because dissolved oxygen is the most efficient triplet quencher[7], this approach increases photo-stability at the expense of triplet state buildup, the main cause of low photon count rates. Our approach to reach microsecond resolution is thus to minimize triplet buildup by keeping the dissolved oxygen in solution (that is, leaving the enzymatic antioxidants out of the cocktail) and also adding Trolox as an additional triplet quencher. We directly targeted the free oxygen radicals that cause photo-oxidative bleaching by using 2-mercaptoethylamine (cysteamine), a known scavenger of singlet oxygen[8] and hydroxyl radicals[9].

To test the performance of the Trolox-cysteamine combination we performed free diffusion single-molecule FRET experiments on macromolecules labeled with Alexa Fluor 488 (A488) as a FRET donor and Alexa Fluor 594 (A594) as an acceptor (both from Invitrogen Molecular Probes) to determine photon throughput of single molecules on the microsecond timescale. In experiments with a short double-stranded B-DNA molecule[10], we detected some high-emission, 100-μs bursts in the presence of oxygen with and without Trolox (**Fig. 1a**), but we did not detect any bursts in the presence of the enzymatic oxygen scavenger plus Trolox[6] (data not shown). This confirmed that oxygen is a most efficient triplet quencher. Without photoprotection or with Trolox alone, however, the high emission bursts were very short (typically <100 μs), indicating that the dyes were quickly bleaching. Accordingly, the resulting FRET efficiency histograms were extremely distorted with a major peak at 0 FRET efficiency and virtually no events showing the 0.55 FRET efficiency expected for the B-DNA molecule (**Fig. 1b**,**c**). With the Trolox-cysteamine mix we observed a dramatic increase in the number of high emission bursts, reaching an about 40-fold increase over Trolox alone at irradiance slightly below saturation (**Fig. 1a**). Moreover, for the Trolox-cysteamine mix, the FRET histogram showed a large peak at the appropriate FRET efficiency with a relatively low 0 FRET efficiency population (**Fig. 1d**). These results demonstrated that cysteamine helps both the donor and acceptor dyes maintain high emission rates for much longer times. We obtained similar results

[1]Centro de Investigaciones Biológicas, Consejo Superior de Investigaciones Científicas, Madrid, Spain. [2]Department of Chemistry and Biochemistry, University of Maryland, College Park, Maryland, USA. [3]Present addresses: Department of Pediatrics, Stanford University, Stanford, California, USA (J.L.), Department of Chemistry, University of North Carolina, Chapel Hill, North Carolina, USA (X.W.) and Department of Chemistry, Wichita State University, Wichita, Kansas, USA (D.S.E.). [4]These authors contributed equally to this work. Correspondence should be addressed to V.M. (vmunoz@cib.csic.es).

RECEIVED 27 APRIL 2010; ACCEPTED 7 DECEMBER 2010; PUBLISHED ONLINE 9 JANUARY 2011; DOI:10.1038/NMETH.1553

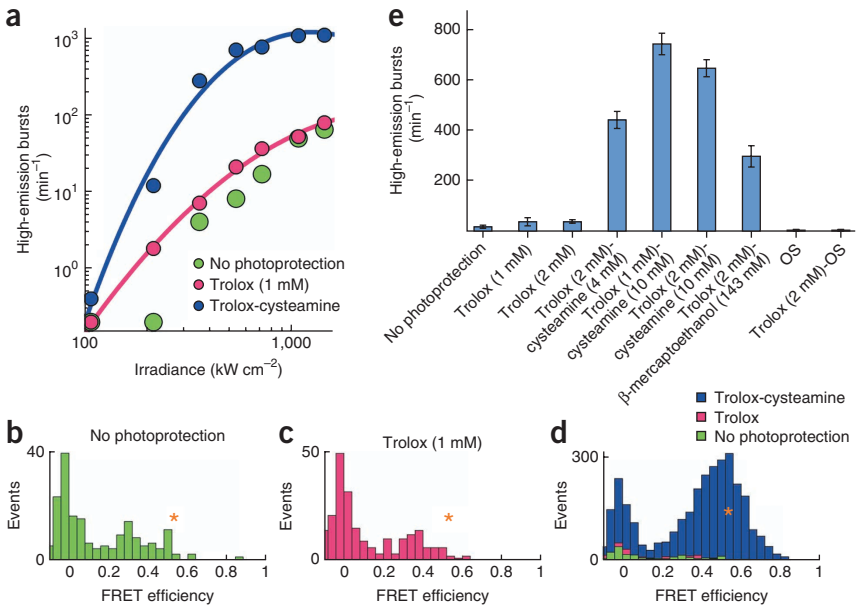

Figure 1 | Effect of photoprotectors on the photon throughput of B-DNA[10] labeled with A488-A594 at 10-base-pair separation. (**a**) We irradiated the DNA with high continuous wave 485-nm laser excitation intensities and collected 100-µs bins with more than 50 total photons (donor plus acceptor) over the background, which we termed high-emission bursts for simplicity. Plotted are the high-emission bursts detected in one minute from free diffusing single molecules. The lines are fits to polynomial functions. Trolox-cysteamine, 1 mM Trolox and 10 mM cysteamine. (**b**–**d**) FRET efficiency histograms calculated from the high-emission bursts collected over a 5-min period with irradiance of 525 kW cm^{-2}. Asterisk, bulk FRET efficiency. (**e**) High-emission bursts min^{-1} at 700 kW cm^{-2} irradiance for indicated combinations of photoprotectors. Error bars, s.d. (five experiments). OS, enzymatic oxygen scavenger as described in reference 6 and Online Methods.

in experiments with A488-A594–labeled proteins (**Supplementary Fig. 1**).

The use of cysteamine as a photoprotector involves a trade-off because its reduced thiol also quenches fluorescence[8]. We confirmed that cysteamine does in fact quench A488 and A594 fluorescence (**Supplementary Fig. 2**). Under high irradiance and below 20 mM cysteamine, however, the protection against photobleaching greatly outweighed the decrease in dye brightness (**Supplementary Fig. 2**). The related compound β-mercaptoethanol had similar effects but proved to be much less efficient (**Fig. 1e**). Other combinations of compounds we tested also performed worse (**Fig. 1e**). Thus we concluded that 1 mM Trolox plus 10 mM cysteamine offered the best performance for achieving microsecond resolution single-molecule FRET with A488 and A594. This Trolox-cysteamine cocktail was less effective on carbocyanine dyes such as the Cy3-Cy5 FRET pair (**Supplementary Fig. 3** and **Supplementary Table 1**), possibly because the emission rates of this pair were dominated by long-lasting blinking

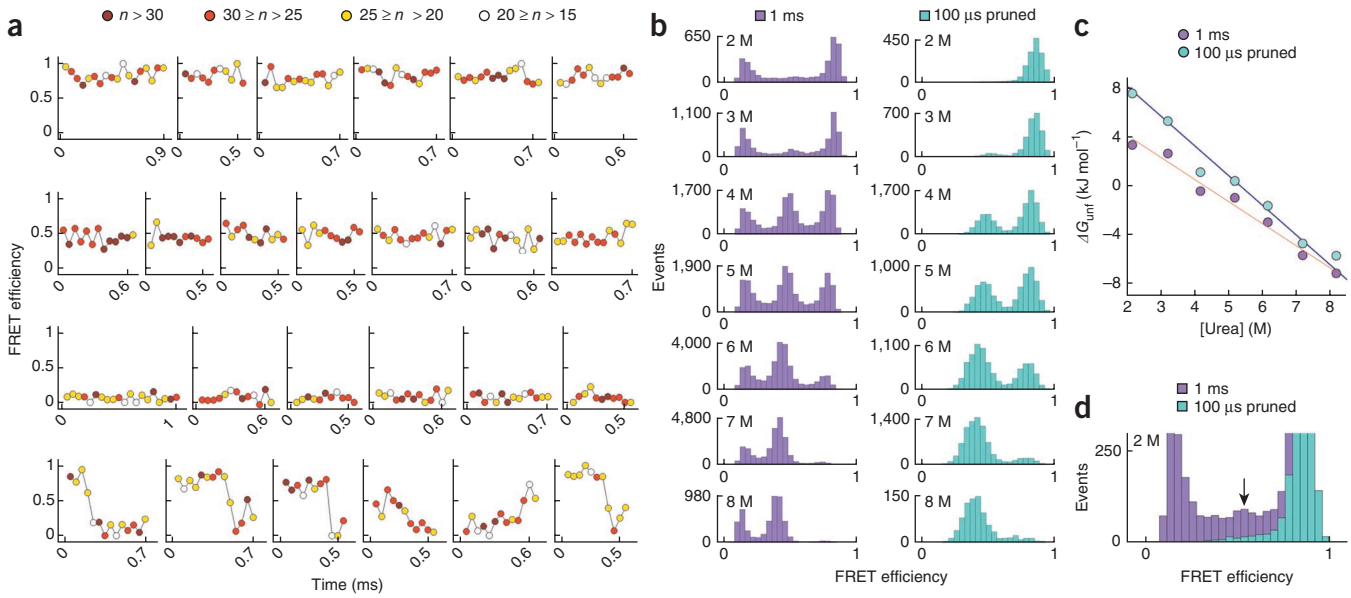

Figure 2 | Microsecond-resolution free-diffusion single-molecule FRET experiments of α-spectrin SH3 domain labeled with A488-A594 on two cysteines introduced at the protein ends. (**a**) Examples of FRET efficiency trajectories of α-spectrin SH3 domain single molecules freely diffusing through the observation volume of the confocal microscope. The time resolution was 50 µs, and colors represent the number of photons (*n*) in each 50-µs bin. Shown are examples of trajectories of folded molecules (~35% of the total; top row); trajectories of unfolded molecules (~40% of the total; second row); trajectories with the acceptor in a dark state (12% of the total; third row); and trajectories that showed bleaching or long-lasting blinking (bottom row). (**b**) FRET-efficiency histograms at indicated urea concentrations obtained from 1-ms bins with >200 photons (left) and from 100-µs bins of >50 photons after pruning all single-molecule diffusive trajectories that visited the (dark-acceptor state) (FRET efficiency values below 0.2) at any point (right). (**c**) Free energy of unfolding as a function of urea concentration calculated from the relative areas of the folded (~0.75 FRET efficiency) and unfolded (~0.4 FRET efficiency) peaks compared to the bulk estimate (dark blue line). The red line shows the linear regression to the single-molecule data obtained with 1-ms binning for reference. (**d**) Comparison of the two FRET-efficiency histograms at 2 M urea expanded to highlight the artifacts in the intermediate FRET-efficiency region.

© 2011 Nature America, Inc. All rights reserved.

coupled to photo-isomerization rather than triplet buildup. This result implied that, in principle, the Cy3-Cy5 pair is not a good option for microsecond single-molecule FRET.

We then applied the Trolox-cysteamine mix together with the A488-A594 pair to resolve the microsecond FRET efficiency fluctuations that occur in free-diffusing single protein molecules. Our goal was to exploit the potential increase in time resolution to test for the existence of conformational dynamics in protein unfolded states, produce more accurate FRET efficiency histograms and resolve the folding-unfolding transitions of fast-folding proteins.

First we looked at the slow two-state folding SH3 domain from the α-spectrin protein (**Supplementary Fig. 4**). Using the Trolox-cysteamine mix, we resolved the FRET fluctuations undergone by diffusing single molecules of α-spectrin SH3 domain with 50-μs resolution (**Fig. 2a**). In experiments near the denaturation midpoint of this protein we observed three kinds of single-molecule trajectories: (i) trajectories with high FRET efficiency corresponding to folded molecules; (ii) trajectories with ~0.45 FRET efficiency signaling unfolded molecules; (iii) trajectories with 0 FRET efficiency indicating that the acceptor is in a dark state or missing. The FRET-efficiency fluctuations were always proportional to the shot-noise level, indicating that α-spectrin SH3 domain did not undergo microsecond to millisecond conformational dynamics in either the folded or unfolded state.

We did not detect folding-unfolding interconversions because the SH3 domain folds and unfolds too slowly, but we observed sharp transitions between either the folded or unfolded states and the dark state (**Fig. 2a**). These transitions represent blinking and bleaching events that would lead to artifacts in FRET-efficiency histograms measured with typical millisecond resolution. However, such photochemical artifacts could presumably be minimized by measuring the histograms with shorter binning times and pruning the trajectories that visit the dark state. To test this, we subjected α-spectrin SH3 domain to various urea concentrations (**Fig. 2b**). The FRET efficiency histograms obtained with conventional 1-ms resolution could resolve the two peaks corresponding to the folded and unfolded states and the progressive conversion from folded to unfolded state as urea concentration increased. However, both peaks were broader than expected from shot noise, and the population of the unfolded state calculated from the area of peaks grossly underestimated SH3-domain stability relative to bulk measurements (**Fig. 2c**). We solved both problems by measuring the histograms using 100-μs bins and pruning the trajectories that showed dark state visits (**Fig. 2b,c**). This analysis also highlighted how bleaching and blinking can produce extra peaks at intermediate FRET values that could easily be confused with molecular species (**Fig. 2d**).

We also applied the Trolox-cysteamine mix to resolve the sub-millisecond conformational dynamics of BBL, an α-helical protein that folds and unfolds in microseconds and has been described as a model of downhill folding[11] (**Fig. 3a**). We performed free-diffusion single-molecule FRET experiments near BBL's chemical denaturation midpoint (5 M urea) at 279K to slow the folding relaxation to times over 100 μs[11]. In this case we obtained peak emissions of ~0.8 MHz, only about fourfold below the theoretical

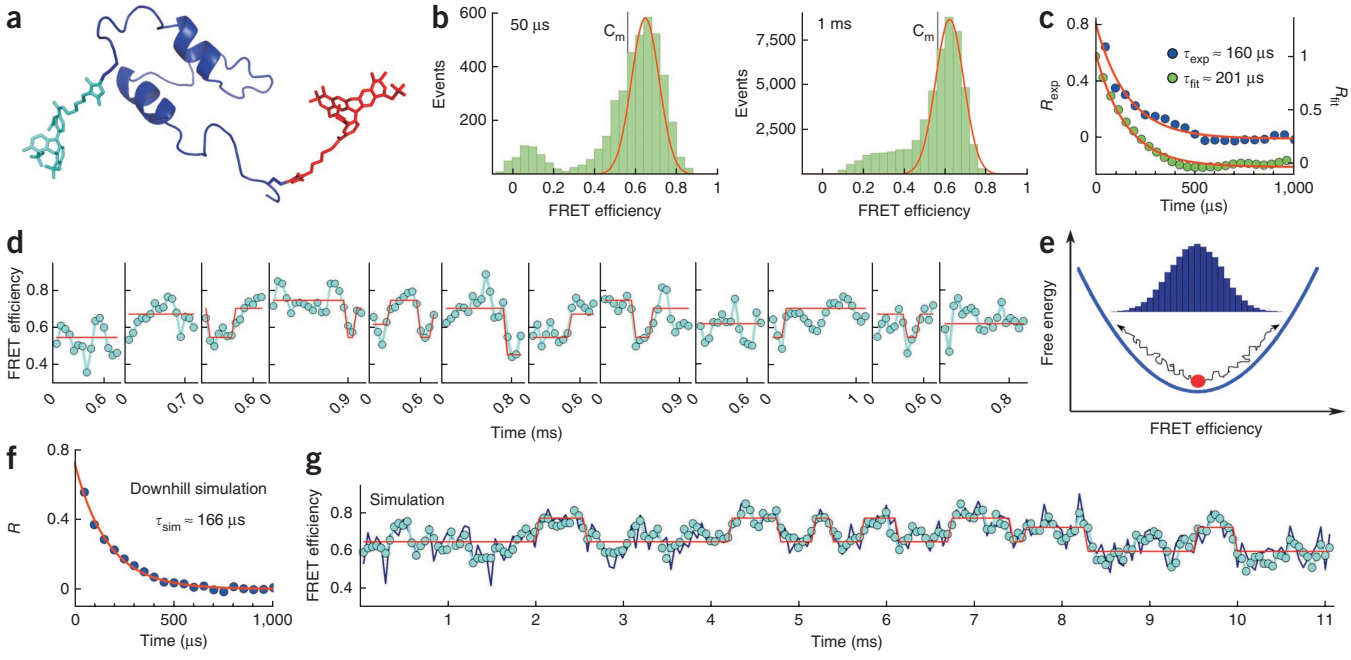

Figure 3 | Microsecond resolution free diffusion single-molecule FRET of BBL. (**a**) A three-dimensional structure of BBL labeled with A488 (cyan) and A594 (red) on the ends of long unstructured tails. (**b**) FRET efficiency histograms of labeled BBL in 5 M urea (the denaturation midpoint (C_m) was ~5.3 M) obtained from 50-μs bins (left) and 1-ms bins (right) with >40 total photons over background. The expected shot-noise width is shown in red and the FRET efficiency value at the C_m is indicated with a black vertical line. (**c**) FRET-efficiency autocorrelation function (R) calculated from experimental free diffusion trajectories (blue) and from the maximum likelihood fit to a seven-states model (green). The red curves are fits to an exponential function with the indicated relaxation times. (**d**) Examples of free-diffusing BBL trajectories near the denaturation midpoint (cyan circles). The red lines show the fit to the seven-states model for each trajectory. (**e**) Cartoon of the stochastic dynamic simulations on a harmonic potential. (**f**) FRET-efficiency autocorrelation function (R) for the downhill simulation. The fit (red curve) to a single exponential function is shown with the relaxation time indicated. (**g**) A 10-ms single-molecule trajectory simulated with the stochastic downhill model sketched in **e**. A simulation of shot-noise corresponding to a 0.8 MHz photon count rate (dark blue) and the fit to the seven-states model (red).

© 2011 Nature America, Inc. All rights reserved.

maximum. The FRET-efficiency histogram calculated with 50-μs bins showed a single, near-Gaussian peak centered at ~0.6 FRET efficiency rather than the classical two peaks for the folded and unfolded states (**Fig. 3b**). The peak position coincided with that in bulk measurements, but the distribution was broader than shot noise. When the data were binned in 1-ms intervals the 0 FRET efficiency peak moved to higher FRET efficiency, indicating that the acceptor bleached on the millisecond timescale (**Fig. 3b**). Notably, the extra width of the peak at 0.6 FRET efficiency disappeared in the 1-ms histogram (**Fig. 3b**), suggesting the presence of sub-millisecond conformational dynamics. We confirmed this point by calculating the autocorrelation function for 137 free-diffusing BBL trajectories without deactivations, which resulted on an exponential decay with relaxation time of ~160 μs that corresponds to the folding-unfolding dynamics of BBL near its denaturation midpoint (**Fig. 3c**). The individual free-diffusing trajectories revealed FRET-efficiency fluctuations of varying timescale and amplitude that were inconsistent with two-state folding (**Fig. 3d**), and suggest either a greater number of FRET-distinguishable states or diffusive trajectories along a shallow free energy surface. In fact, a maximum likelihood analysis identified transitions between at least seven different states. Moreover, the model with seven states still missed some FRET dynamics as it was apparent by visual inspection (**Fig. 3d**) and from the slower decay of the autocorrelation function of the fits to the seven-states model (**Fig. 3c**).

The single-molecule folding-unfolding dynamics of BBL revealed stochastic patterns reminiscent of the diffusive Brownian motions that are purportedly the signature for downhill folding[12]. We explored this idea by building a simple theoretical model that describes downhill folding as diffusion on a single welled one-dimensional free-energy surface (**Fig. 3e**). We first parameterized the model to reproduce the experimental autocorrelation function (**Fig. 3f**) and then carried out stochastic simulations of single-molecule trajectories (Online Methods). These simulations showed FRET fluctuations of the same timescales and amplitudes as those observed experimentally (**Fig. 3g**). Such similarities become even more apparent after comparing the simulations with their fit to the seven-states model, which again missed part of the dynamics. A detailed analysis of BBL folding dynamics is beyond the scope of this work. However, these experiments unambiguously demonstrate that single-molecule FRET methods can be used to resolve the conformational fluctuations of microsecond folding proteins in free-diffusion experiments.

There are now several methods to access sub-millisecond conformational motions of macromolecules in bulk using either fluorescence detection[13] or nuclear magnetic resonance[14]. The combination of fluorescence-correlation spectroscopy and contact quenching can even reach the single-molecule detection limit[15]. However, all these methods measure collective relaxation decays that need to be interpreted with kinetic models. In contrast, the single-molecule FRET approach we introduce here resolves the time-dependent conformational fluctuations of single molecules with microsecond resolution. It can be used for proteins and nucleic acids, and works best with dyes that do not undergo long-lasting blinking by *cis-trans* isomerization such as the A488-A594 pair. This approach opens a direct avenue for studying, at the single-molecule level, a vast array of biological processes that are either controlled or mediated by sub-millisecond macromolecular motions. Some examples among these include the dynamics of enzymes during catalytic turnover, the conformational changes of molecular switches, the sliding-search motions that take place in macromolecular encounter complexes and the entire folding process of the growing number of identified ultrafast folding proteins.

METHODS

Methods and any associated references are available in the online version of the paper at http://www.nature.com/naturemethods/.

Note: Supplementary information is available on the Nature Methods website.

ACKNOWLEDGMENTS

This research was supported in part by the Marie Curie excellence grant MEXT-CT-2006-042334 and grants BFU2008-03237 and CONSOLIDER CSD2009-00088 from the Spanish Ministry of Science and Innovation.

AUTHOR CONTRIBUTIONS

L.A.C. and J.L. prepared samples, identified the oxygen radical scavengers, performed experiments and analyzed data. L.A.C. performed all the additional experiments requested by the reviewers. X.W. acquired and analyzed data. R.R. performed the stochastic simulations of downhill folding. D.S.E. supervised data acquisition and designed research. V.M. designed research, supervised data acquisition, performed and supervised data analysis and simulations, and wrote the manuscript.

COMPETING FINANCIAL INTERESTS

The authors declare no competing financial interests.

Published online at http://www.nature.com/naturemethods/.
Reprints and permissions information is available online at http://npg.nature.com/reprintsandpermissions/.

1. Moerner, W.E. *Proc. Natl. Acad. Sci. USA* **104**, 12596–12602 (2007).
2. Roy, R., Hohng, S. & Ha, T. *Nat. Methods* **5**, 507–516 (2008).
3. Schuler, B. & Eaton, W.A. *Curr. Opin. Struct. Biol.* **18**, 16–26 (2008).
4. Gell, C., Brockwell, D. & Smith, A. *Handbook of Single Molecule Fluorescence Spectroscopy*. (Oxford University Press, 2006).
5. Kong, X.X., Nir, E., Hamadani, K. & Weiss, S. *J. Am. Chem. Soc.* **129**, 4643–4654 (2007).
6. Rasnik, I., McKinney, S.A. & Ha, T. *Nat. Methods* **3**, 891–893 (2006).
7. Turro, N.J. *Modern Molecular Photochemistry*. (University Science Books, 1991).
8. Dittrich, P.S. & Schwille, P. *Appl. Phys. B* **73**, 829–837 (2001).
9. Misik, V., Miyoshi, N. & Riesz, P. *Free Radic. Biol. Med.* **26**, 961–967 (1999).
10. Wozniak, A.K., Schroder, G.F., Grubmuller, H., Seidel, C.A. & Oesterhelt, F. *Proc. Natl. Acad. Sci. USA* **105**, 18337–18342 (2008).
11. Li, P., Oliva, F.Y., Naganathan, A.N. & Muñoz, V. *Proc. Natl. Acad. Sci. USA* **106**, 103–108 (2009).
12. Muñoz, V. *Annu. Rev. Biophys. Biomol. Struct.* **36**, 395–412 (2007).
13. Eaton, W.A. *et al. Annu. Rev. Biophys. Biomol. Struc.* **29**, 327–359 (2000).
14. Fawni, N.L., Douclef, M., Suh, J.Y. & Clore, M.G. *Proc. Natl. Acad. Sci. USA* **107**, 1379–1384 (2010).
15. Neuweiler, H., Johnson, C.M. & Fersht, A.R. *Proc. Natl. Acad. Sci. USA* **106**, 18569–18574 (2009).

© 2011 Nature America, Inc. All rights reserved.

ONLINE METHODS

Reactants, samples and procedures. The photoprotection cocktail used in these studies contained 1 mM (S)-Trolox methyl ether and 10 mM 2-mercaptoethylamine (cysteamine). Both compounds and mercaptoethanol, were purchased from Sigma-Aldrich. The enzymatic oxygen scavenger cocktail used for comparison experiments was composed of 0.4% w/w glucose, 165 U ml^{-1} of glucose oxidase (Sigma) and 2170 U ml^{-1} of catalase (Sigma) following the original recipe[6].

Production of fluorescently labeled macromolecules. The α-spectrin SH3 domain sequence was slightly modified for labeling purposes, adding a cysteine together with two lysines at each protein end. Lysines were added to introduce tail flexibility with the goal of reducing fluorophore-protein interactions and increasing thiol reactivity. The sequence of the final protein construct was MACKKDETGKELVLALYDYQEKSPREVTMKKGDILTLL NSTNKDWWKVEVNDRQGFVPAAYVKKLDGKKC.

The BBL sequence was modified for labeling, extending both unstructured tails based on the original gene sequence and adding two lysines before the cysteine on each end: MDCKKNNDALSPA IRRLLAEHNLDASAIKGTGVGGRLTREDVEKHLAKAPAKKC. For protein experiments, we used A488 as donor and A594 as acceptor (Invitrogen Molecular Probes).

Protein samples were labeled following the protocol provided by the manufacturer. We labeled the donor first, purified the protein labeled with a single donor from the reaction mixture, and then labeled to saturation with the acceptor followed by purification of the donor and acceptor–labeled protein. The different species from the reaction mixture were separated or purified using reverse-phase high-performance liquid chromatography on a C18 preparative column. Sample purity was confirmed by matrix-assisted laser desorption/ionization mass spectrometry analysis.

For DNA experiments, we purchased from IBA four different single stranded DNA sequences labeled with the appropriate dyes: 5′-TAAGGCGATCT$_x$CTGT-3′ labeled with A488 or Cy3 at T$_x$ position and 5′-ACAGAGATCGCCTTA$_x$-3′ labeled with A594 or Cy5 in A$_x$ position.

Free-diffusion single-molecule FRET (smFRET) experiments. smFRET measurements were carried out using either a custom-made single-molecule fluorescence microscope system previously described[16] or a MicroTime 200 (PicoQuant). A488 excitation was achieved with either the 488 nm line of a continuous wave (CW) argon ion laser or a LDH-D-C485 (485 nm ± 10 nm) (PicoQuant) run in CW mode. Cy3 excitation was achieved at 532 nm using a solid-state CW Gem 25-mW laser (Laser Quantum).

All macromolecule samples were prepared at 75 pM concentration for all single-molecule experiments. SH3-domain experiments were performed at 298K in 20 mM acetate buffer (pH 5). BBL experiments were performed at 279K in 20 mM acetate buffer (pH 6). B-DNA experiments were performed at 298K in 50 mM Tris buffer (pH 7.6) with 150 mM NaCl, 1 mM EDTA, 5 mM $MgCl_2$ and 0.4 mM ascorbic acid following the conditions previously described[10]. We checked for possible double-molecule events by looking at the photon-counting histograms[17] and then discarding any burst with photon emissions >2σ higher than the average.

Data analysis and simulations. The original smFRET data were acquired collecting photons with 50-μs acquisition time. Longer binning times were produced combining the corresponding number of consecutive 50-μs bins required to obtain the desired binning time. FRET efficiency (*ET*) was obtained using the equation:

$$ET = \frac{S_a - \left(x/(1-x)\right)S_d}{S_a + S_d}$$

in which S_a and S_d are the number of photons detected in the acceptor and donor channel after subtracting the background, and x is the fraction of donor photons that leak through to the acceptor channel (corresponding to 0.08). In **Supplementary Figure 1**, smFRET efficiency was calculated by simple ratiometry as $ET = S_a / (S_a + S_d)$, where S_a and S_d are the number of photons detected in the acceptor and donor channel signals, respectively.

Data were analyzed using Matlab (MathWorks) and Origin (OriginLab).

The free-diffusing single-molecule trajectories of BBL were analyzed with a maximum likelihood approach that uses a hidden Markov model and by stitching all free-diffusion trajectories into a single trace as recommended previously[18]. Different stitching arrangements were tried to rule out any artifacts from the stitching procedure. All models from two up to ten states were attempted, but the analysis with seven states gave the maximum likelihood and the best fit to the stitched trajectory.

The dynamics of downhill folding as diffusion on a single welled free energy surface were simulated using a 100-point discretized harmonic potential of the form $F = -RT \ln(p)$, where p is the probability of any given FRET efficiency value obtained from a Gaussian distribution with mean of 0.66 and s.d. of 0.075. The discretized diffusion master equation was obtained using the matrix method[19]. Single-molecule stochastic trajectories were simulated by moving on the harmonic well in single steps according to the following time-dependent probabilities:

$$p\left(i \to i+1\right) = \Delta t \frac{1}{2}\left(\frac{p_{i+1}}{p_i}D + D\right)$$

$$p\left(i \to i-1\right) = \Delta t \frac{1}{2}\left(\frac{p_{i-1}}{p_i}D + D\right)$$

$$p\left(i \to i\right) = 1 - \left(p\left(i \to i+1\right) + p\left(i \to i-1\right)\right)$$

in which D is the intramolecular diffusion coefficient and Δt is small enough to guarantee that the probability of jumping to either of the flanking states is always <0.1.

16. Morgan, M.A., Okamoto, K., Kahn, J.D. & English, D.S. *Biophys. J.* **89**, 2588–2596 (2005).
17. Gopich, I.V. & Szabo, A. *J. Phys. Chem. B* **109**, 17683–17688 (2005).
18. McKinney, S.A., Joo, C. & Ha, T. *Biophys. J.* **91**, 1941–1951 (2006).
19. Lapidus, L.J., Steinbach, P.J., Eaton, W.A., Szabo, A. & Hofrichter, J. *J. Phys. Chem. B* **106**, 11628–11640 (2002).

© 2011 Nature America, Inc. All rights reserved.